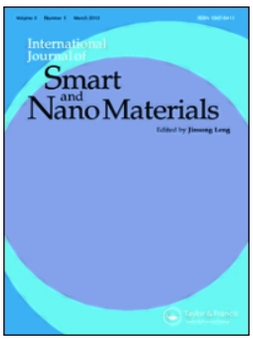

International Journal of Smart and Nano Materials

ISSN: (Print) (Online) Journal homepage: https://www.tandfonline.com/loi/tsnm20

The wrinkle formation in graphene on transition metal substrate: a molecular dynamics study

Chao Zhao , Fengning Liu , Xiao Kong , Tianying Yan & Feng Ding

To cite this article: Chao Zhao , Fengning Liu , Xiao Kong , Tianying Yan & Feng Ding (2020) The wrinkle formation in graphene on transition metal substrate: a molecular dynamics study, International Journal of Smart and Nano Materials, 11:3, 277-287, DOI: 10.1080/19475411.2020.1820621

To link to this article: https://doi.org/10.1080/19475411.2020.1820621

Published online: 11 Sep 2020.

INTERNATIONAL JOURNAL OF SMART AND NANO MATERIALS
2020, VOL. 11, NO. 3, 277–287
https://doi.org/10.1080/19475411.2020.1820621

Taylor & Francis
Taylor & Francis Group

ARTICLE

The wrinkle formation in graphene on transition metal substrate: a molecular dynamics study

Chao Zhao[a,b], Fengning Liu[a,b], Xiao Kong[b], Tianying Yan[c] and Feng Ding[a,b]

[a]School of Materials Science and Engineering, Ulsan National Institute of Science and Technology (UNIST), Ulsan, Republic of Korea; [b]Center for Multidimensional Carbon Materials, Institute for Basic Science, Ulsan, Republic of Korea; [c]Institute of New Energy Material Chemistry, School of Materials Science and Engineering, National Institute for Advanced Materials, Nankai University, Tianjin, P. R. China

ABSTRACT

To explore the mechanism of the wrinkle formation in graphene on transition metal substrate, a molecular dynamics (MD) simulation package that allows us to simulate systems of millions of atoms was developed. Via the MD simulation, we reveal the detailed kinetics of wrinkles formation on a Cu substrate under compressive strain, from nucleation to one-dimensional propagation and then the splitting of a large wrinkle to a few smaller ones, which is in good conformity with experimental observation. Further study reveals that both friction and the adhesion between graphene and Cu substrate are critical for the wrinkle formation and wrinkles can be easily formed with a lower frictional force and/or a smaller adhesion. Finally, we have shown that impurities in graphene or substrates can greatly facilitate the nucleation of wrinkles. The systematic exploration of the wrinkle formation in graphene on a substrate is expected to facilitate the experimental designs for the controllable synthesis of high-quality graphene.

ARTICLE HISTORY
Received 12 May 2020
Accepted 6 July 2020

KEYWORDS
Graphene; wrinkles; molecular dynamic simulation; chemical vapor deposition

1. Introduction

Graphene as a two-dimensional material has many unique physical and mechanical properties, including highest strength and elastic stiffness, in-plane electrical conductivity, thermal conductivity, and optical absorption which results in many potential applications in mechanical, electronic, and photonic devices [1–8]. Currently, chemical vapor deposition (CVD) is the widely employed method to produce graphene in large areas and high quality at a reasonable lower price [9–12]. As we cool down the system from the temperature of graphene CVD growth (~ 1000°C) to room temperature, wrinkles are formed due to the compressive strain in graphene induced by the larger thermal expansion of the substrate than that of graphene [13–17]. Graphene wrinkles may greatly degrade the carrier mobility [18], mechanical strength [19], thermal conductivity [20], and strain sensitivity of the CVD graphene in applications [21]. Hence, understanding the formation mechanisms of wrinkling induced by the compressive strain is highly desired for controllable graphene synthesis.

CONTACT Feng Ding f.ding@unist.ac.kr gniding@gmail.com Center for Multidimensional Carbon Materials, Institute for Basic Science, Ulsan 44919, Republic of Korea

In 2015, de Lima, Amauri Libério, et al. [22] developed an analytical model with considering the binding and bending energies to analyze the criterion of wrinkle formation in graphene and have found that ~2.8% compressive strain is required to initiate a wrinkle in a perfect graphene layer on the top of another graphene layer. Baowen Li et al. [23] proposed a wrinkle nucleation model by considering the bending stiffness of graphene, adhesion between graphene and Cu substrate, and the friction force of graphene sliding on Cu surface and successfully explained that the reference of wrinkle formation in the non-epitaxial graphene region is mainly induced by smaller friction force than that of the epitaxial graphene. Wen Wang et al. [1] adopted MD simulations to explain the enlarged wrinkles on the copper substrate and Zhenqian Pang et al. [14] reported how the Stone–Wales defects and grain boundaries influence the wrinkle formation in graphene on different copper substrates using the large-scale atomic/molecular massively parallel simulator (LAMMPS) [24]. Moreover, Kuan Zhang et al. [25,26] developed a continuum model to understand how strain anisotropy, adhesion, and friction govern spontaneous wrinkling of graphene on a substrate.

So far, the analytical models, density functional theory calculations, classical MD simulations, and continuum models are all used to study the wrinkling formation in a thin film on a substrate. But the wrinkle formation on transition metal substrates has never been systematically explored, such as how the friction, adhesion, and defects affect the formation of wrinkles and, especially, the comparison with experimental observations was rarely explored. In this paper, we firstly introduce the growth procedures and characterization of wrinkles in graphene grown on Cu surface in a CVD process. Then, details of the computational methods and parameterizations are presented. As an example, we presented a detailed wrinkle formation process during the increase of the compressive strain with atomic details. Finally, the influences of the friction, adhesion, and the defects in graphene and substrate on wrinkle formation are explored.

2. Experimental details

2.1 Graphene growth on the polycrystalline copper foil

Graphene grows on polycrystalline copper foil by the Chemical Vapor Deposition method. The copper foil was first heated to 1050°C in 60 minutes under H_2 gas flow at 2 Torr pressure. Then, 30 sccm diluted CH_4(1% CH_4 in Ar gas) and 300 sccm H_2 gas was introduced into the chamber for 1 h. After growth, the furnace was removed to force copper foil to cool down under the same gas flow and pressure as the growth period.

2.2 Characterization

SEM was performed with FEI Verios 460 SEM, and AFM data was acquired with the Bruker Dimension Icon system.

3. Computational details

3.1 Description of the force field for the carbon-metal interactions

So far, the C-C interaction was successfully described by the second-generation reactive empirical bond order (REBO) potential [27], which is based on the Tersoff [28] and Tersoff-Brenner potential [29]. But to a better description of some particular C-C interactions, a parameter a_{ij} was introduced to weaken the C-C interaction in the following form [30,31]:

$$E_{ij} = a_{ij}\left[V^R(r_{ij}) - V^A(r_{ij})\right] \tag{1}$$

in which the $V^R(r_{ij})$ is the repulsive term and $V^A(r_{ij})$ is the attractive interaction term. The Cu-Cu interaction in the copper substrate was described by the embedded atom method (EAM) potential, which has been successfully explored the structural properties of Cu, Ag, Au, Pd, Ni, and Pt as well as alloys containing these metals [32]. The C-Cu interaction was characterized by the Lennard–Jones (L-J) '12–6' potential [33] to study the adhesion and friction effects by adjusting the parameters ε and σ which are presented in the following equation:

$$U_{vdw}(r) = 4\varepsilon\left[\left(\frac{\sigma}{r}\right)^{12} - \left(\frac{\sigma}{r}\right)^{6}\right] \tag{2}$$

where ε and σ, respectively, characterize the depth of the potential well and the equilibrium position of atomic distance, and r is the distance between atomic pairs.

3.2 Parameters fitting for the C-Cu interaction

In the atomistic simulation, two types of systems were considered, monolayer graphene on single-layer rigid Cu substrate and monolayer graphene on multi-layers Cu slab with the atoms of the bottom layer fixed, which are presented in Figure 1(a,b). For different equilibrium positions of atomic distance (σ), the L-J potential parameter (the potential well depth (ε)), are fitted with the calculated C-Cu adhesion energy of ~35 meV/C atom [34]. Figure 1(c) shows the L-J potential well depth (ε) as functions of graphene-copper

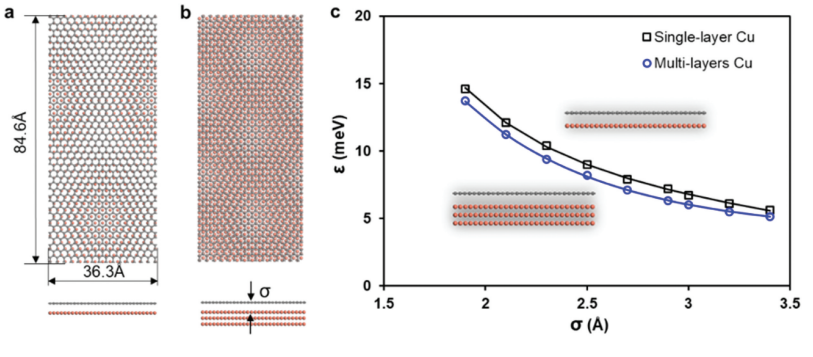

Figure 1. a) Atomic model of graphene on a single-layer Cu substrate. b) Atomic model of graphene on multi-layers Cu substrate. c) Parameters fitting of the classical Lennard-Jones potential for monolayer graphene on single-layer and multi-layers Cu substrate.

distance (σ). The graphene–copper interactions for single-layer and multi-layers Cu substrate are defined as

$$E_{Gr-SLCu} = \frac{\left[E_{Gr} - E_{Gr/Cu}\right]}{N} \tag{3a}$$

$$E_{Gr-MLCu} = \frac{\left[E_{Gr} + E_{Cu} - E_{Gr/Cu}\right]}{N} \tag{3b}$$

Where E_{Gr}, E_{Cu}, $E_{Gr/Cu}$ represent the energies of free-standing graphene, the Cu substrate, and the graphene at the Cu surface, respectively. The parameter N is the number of C atoms. We found that the L-J potential well depth (ε) decreases with the graphene-copper distance (σ) increasing for both single-layer and multi-layers Cu systems.

3.3 Frictional force of graphene sliding on the Cu substrate

To study the effect of friction force on wrinkle formation, the friction of the graphene sliding on the substrate must be calculated. Herein, we proposed three approaches to calculate the frictional force between the graphene and the Cu substrate and the schematic illustrations of them are shown in Figure 2(a-c), in which the red and gray color represents the Cu and graphene, respectively. The first approach is to slide a graphene sheet on the Cu substrate with a constant velocity (Figure 2(a)). The dimensions of the graphene and Cu substrate are 80 $\times$ 3.6 nm^2 and 100 $\times$ 3.6 nm^2, respectively. The second model sliding the graphene on the multi-layer Cu substrate (Figure 2(b)). The last approach starts with a small graphene sheet with initial velocity on a multi-layer Cu substrate and the friction force can be calculated based on the sliding distance (Figure 2(c)). Finally, the relationship between the frictional force per area and the graphene-copper distance (σ) is established, as shown in Figure 2(d). The friction forces calculated by the three approaches are very close to each other, which validates the computational methods. With the same adhesion energy (35 meV), the friction can be changed drastically by tuning the distance between the graphene layer and the substrate, which allows us to explore the effect of friction force on graphene wrinkle formation. In this MD simulation, a canonical ensemble (NVT) was employed with the temperature fixed via a Nose-Hoover

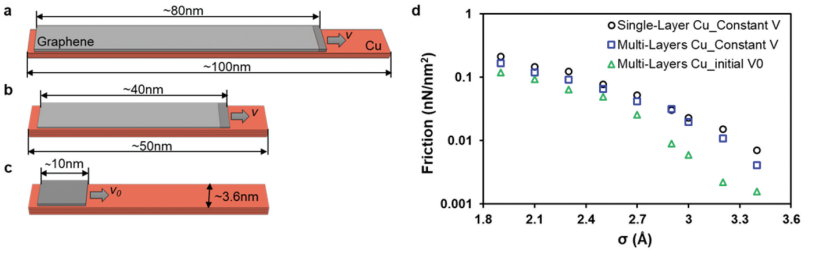

Figure 2. a, b) Models for calculating the frictional force of graphene on single-layer and multi-layers Cu substrate by sliding the graphene with a given velocity, respectively. c) The model of calculating the frictional force of graphene on the multi-layers Cu substrate under a given initial velocity. d) The variation of frictional force per area with different distances between the graphene and Cu substrate.

thermostat (T = 300 K) [35]. Each MD simulation ran for 100 ps at a time step of 1 fs. Furthermore, the periodical boundary condition was utilized in these three models.

3.4 MD simulation details for wrinkle formation

The wrinkle formation mainly depends on the interactions between the graphene sheet and the first layer of Cu substrates, including the friction force and the adhesion energy. As shown in Figure 2(b), the friction force difference of the graphene sliding on the single-layer and multi-layers Cu substrates, respectively, is very small if the same adhesion energy (35 meV/C atom) is considered. So, both models can be used to explore the formation of wrinkles in graphene on Cu surface properly. In order to save computational time, we perform MD simulations with a graphene sheet on a single-layer rigid Cu substrate, the size of the atomic model is about 50 $\times$ 100 nm^2 with the periodical boundary condition applied and the total number of atoms is 278,600. This system was coupled to a Nose-Hoover thermostat to maintain at a temperature of 1 K. The uniaxial strain was applied gradually, the compressive strain increases by 0.1% every 10 ps during the simulation.

4. Results and discussion

4.1 Wrinkles in monolayer graphene grown on Cu surface: experimental observations and atomic simulation

The graphene was grown on the polycrystalline copper foil by the CVD method, the detailed description was discussed in Section 2. As we cool down the system from the CVD temperature to room temperature, the wrinkles or folds were observed in graphene. Figure 3(a) presents the SEM image of a graphene island on a copper foil, in which the white and black arrows represent the wrinkles and folds, respectively, and the top-right enlarged SEM image represents the splitting of a graphene wrinkle. The splitting phenomena were found at the ends of both folds and wrinkles. As shown in Figure 3(b), a graphene wrinkle was visualized using AFM morphology imaging. The height profiles of the wrinkles are shown in Figure 3(c-e). Because the Cu substrate is not flat, we roughly got the height values of these wrinkles being ~3.68 nm, 0.7 nm, and 0.6 nm, respectively.

To explain the experimental observations, the MD simulation for wrinkle formation was performed. In this simulation, we took σ = 2.1 Å and ε = 0.012 eV. The C-Cu distance (σ = 2.1 Å) and the potential well depth were fitted by the estimated friction force between graphene and Cu(111) surface (0.096 ~ 0.22 nN/nm^2) reported in Ref [23] and the C-Cu adhesion energy (35 meV/C atom) reported in Ref [34]. Based on the MD simulation, we found that a wrinkle starts to form at the compressive strain 3.2%, which is larger than that of ~2.8% in graphene due to the thermal mismatch [36]. That was because the parameters (ε, σ) we adopted induces a high friction force of graphene sliding on the Cu substrate and the ignorance of the defects in both graphene and substrate. Figure 4 shows the variation of the wrinkle amplitude and energy per C atom as a function of MD step. As we can clearly see that the energy of the system keeps decreasing as the wrinkle height becomes larger and larger. Finally, a constant wrinkle height, ~1.6 nm, is reached after the full relaxation of the compressive strain. For a better

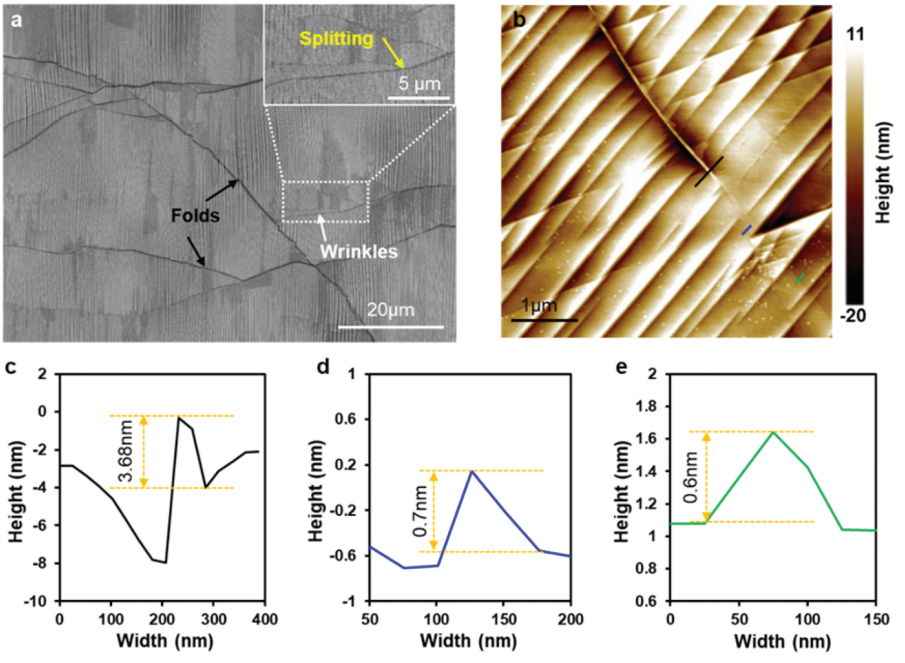

Figure 3. a, b) Characterization of graphene wrinkles on the Cu substrate by SEM and AFM, respectively. c, d, e) The AFM heights of the cross-section trace of the line marked inFigure 3b

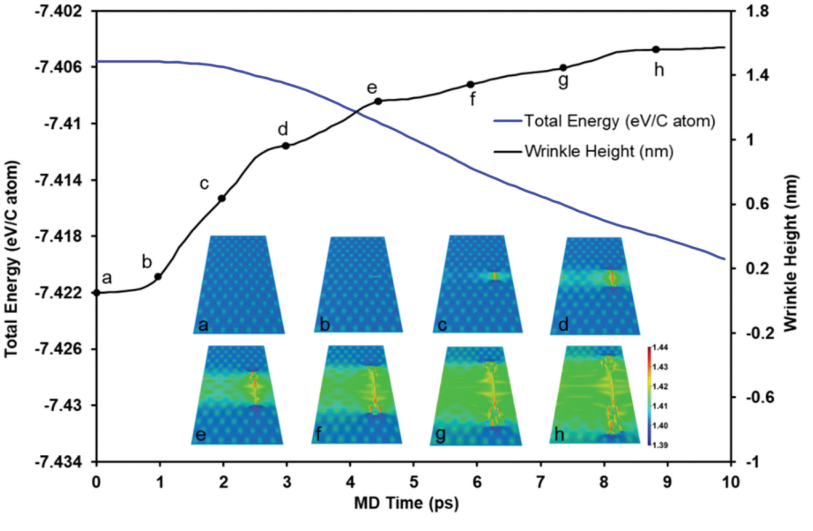

Figure 4. Wrinkle formation process in graphene on single-layer Cu substrate. a-h) shows the morphology of graphene observed during the MD simulation, in which the color represents the bond length distribution of graphene.

understanding of the wrinkle formation, the morphologies of graphene at serval typical MD steps are shown in Figure 4(a-h), in which the color represents the bond length distribution of graphene. Figure 4(a) shows the C-C bond length distribution in a regular

moiré pattern caused by the lattice mismatch between the graphene and the Cu substrate. Firstly, as a critical step of forming a wrinkle, the wrinkle nucleation was observed (Figure 4(b)). Then, the small nucleus of the wrinkle propagates quickly along the direction perpendicular to the compressive strain (Figure 4(c-h)). Finally, the splitting of the wrinkles was observed and there is no further propagation of the existing wrinkle, which is in good agreement with the experimental observation (Figure 3(a)). The wrinkle splitting mainly caused by the strain concentration. As a wrinkle becomes higher and higher, the local strain concentration at the ends of wrinkles will lead to the wrinkle splitting for faster strain relaxation. Moreover, during the nucleation stage, the C-C bond length near the wrinkle position is the largest, implying the relaxation of the compressive strain is the driving force of wrinkle formation.

4.2 Friction and adhesion effect on the wrinkle formation

Here we consider the effect of friction force and the adhesion energy on the formation of graphene wrinkles. To explore the effect of friction force, we consider the system of graphene on the Cu surface, where a constant adhesion energy (35 meV/C atom) is used and the friction force is tuned by varying the C-Cu bond length (σ). The detailed parameters for models are: σ = 2.1 Å, E_a = 35 meV/C atom (f = 0.119 nN/nm^2); σ = 2.7 Å, E_a = 35 meV/C atom (f = 0.039 nN/nm^2); σ = 3.4 Å, E_a = 35 meV/C atom (f = 0.004 nN/nm^2), where f and E_a represent the friction per unit area and adhesion energy/C atom, respectively. The simulation results are shown in Figure 5(a), from which we can see that the critical strain that initiates the wrinkle formation decreases from ~3.2% to ~2.6% with the increase C-Cu bond length or the decreased friction force. As discussed in the previous study, such a change is mainly due to the energy required to slide the graphene on the Cu surface in order to form wrinkles at a specific site. Besides, we found that the initial wrinkle height increases slightly as C-Cu distance decreases. This is due to the release of more compressive strain from the highly compressed graphene. With a brief estimation, we can see that the wrinkle height is determined by the released compressive strain and it is because that the relatively small friction force is not sufficient to main a large compressive strain in the graphene layer after a wrinkle is formed. Figure 5(b) shows the change of the

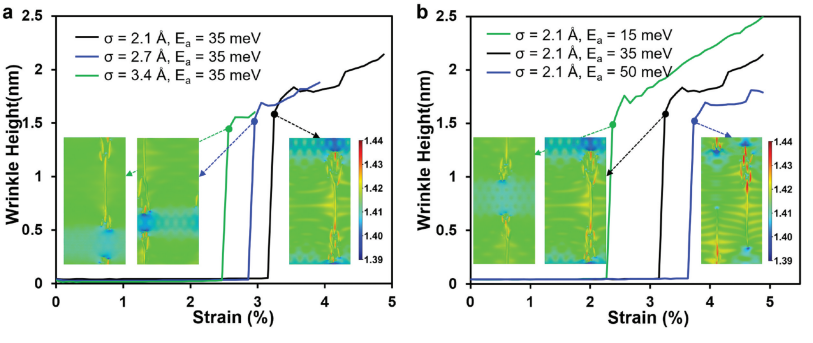

Figure 5. a) The C-Cu distances effect on the wrinkle formation in graphene on the single-layer rigid Cu substrate with a fixed adhesion energy (35 meV/C atom). b) Adhesion effects on the wrinkle formation in graphene on the single-layer rigid Cu substrate with given same C-Cu distances.

critical strain by varying the adhesion energy with given the same C-Cu distances. Three types of models are considered: σ = 2.1 Å, E_a = 15 meV/C atom (ε = 0.005 eV); σ = 2.1 Å, E_a = 35 meV/C atom (ε = 0.012 eV); σ = 2.1 Å, E_a = 50 meV/C atom (ε = 0.017 eV). As expected, the critical strain becomes larger when the adhesion energy was increased, which is in good agreement with the previous analysis [37].

4.3 The effects of defects in graphene and/or substrate on the wrinkle formation

Precious discussions presented a very large critical strain for initiating the wrinkles. Experimentally, the compressive strain due to the cooling of a Cu substrate from the graphene growth temperature (~ 1000°C) to room temperature is ~2.8% and the wrinkles in graphene were observed at 700°C [38]. So, the critical strain must be much smaller than what is shown above. Considering that a large CVD graphene always has many wrinkles and the substrate is hardly to be perfect, we believe the defects in graphene and/or substrate may facilitate the formation of a wrinkle by reducing the nucleation barrier [14,39]. To preliminarily explore the effect of defects in graphene and substrate, we consider an ad-dimer (7|5/5|7) in graphene and an adatom on Cu surface. Figure 6(a) shows the schematic and atomic illustration of ad-dimer defects in graphene and an adatom on Cu substrate beneath the graphene layer. The

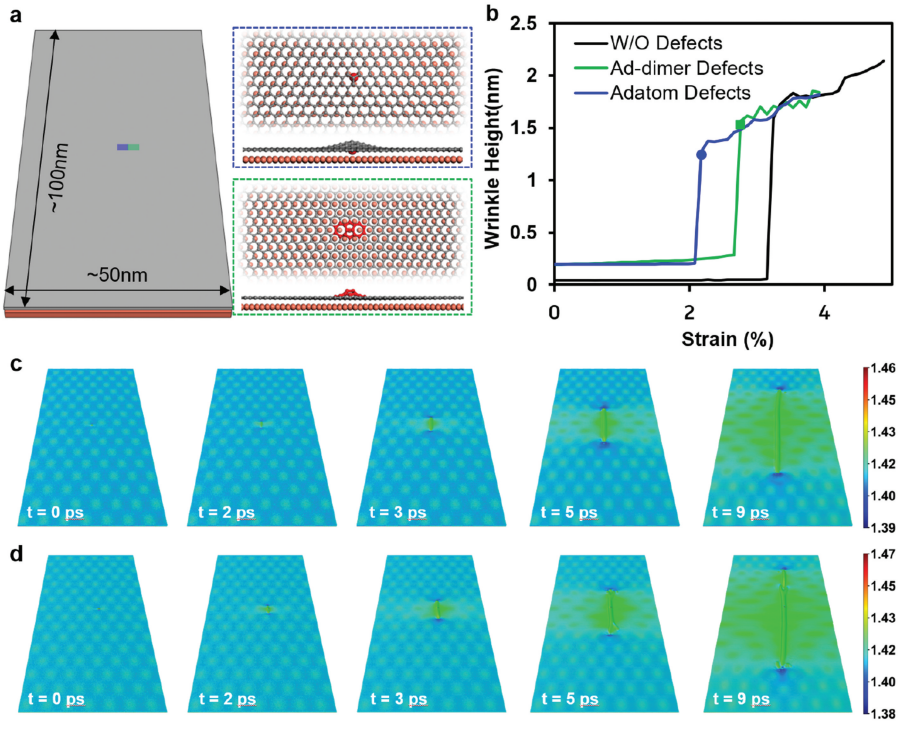

Figure 6. a) The models of an ad-dimer in graphene and an adatom on Cu substrate. b) The effects of an ad-dimer in graphene and an adatom on Cu surface on the wrinkle formation in graphene on Cu substrate with given the parameters σ = 2.1 Å, ε = 0.012 eV, which ensures E_a = 35 meV/C atom. c, d) The graphene wrinkle formation processes on Cu substrate with an adatom on a substrate and an ad-dimer in graphene, respectively.

position of adatom defect in Cu and that of an ad-dimer defect in graphene are presented in blue and green areas on the left side of Figure 6(a), respectively. The enlarged atomic illustrations of the adatom defect and ad-dimer defect are shown in the blue and green boxes on the right side of Figure 6(a,b) presents the comparison of wrinkle height vs. compressive strain curves obtained by simulating the perfect graphene on a flat Cu surface, defect-free graphene on Cu surface with an adatom, and graphene with an ad-dimer on a flat Cu surface, respectively. It is found that both the ad-dimer in graphene and the adatom of the Cu surface greatly reduced the critical strain by 0.6% and 1.1%, respectively. Due to the defects of ad-dimer in graphene and adatom in Cu substrate, part of the graphene was lifted off from the substrate, which prompts the wrinkle nucleation and, therefore, decreases the critical compressive strain of wrinkle nucleation. Figure 6(c,d) demonstrate the wrinkle formation processes in graphene on Cu substrate with an adatom and graphene with ad-dimer at different strains, marked by blue and green dots in Figure 6(b), respectively. From both simulations, we found that wrinkles always start to nucleate at the positions of defective sites, then propagate along the direction that is perpendicular to the direction of strain.

5. Conclusions

We present an in-house-developed MD simulation package that allows us to study the formation mechanism of graphene wrinkles on a transition metal substrate and some preliminary results of wrinkle formation in graphene grown by the CVD method. As observed in our simulation, a complete wrinkle formation process includes wrinkle nucleation, wrinkle propagation, and wrinkle splitting. Then, the relationship between the friction force and the graphene-copper distance (σ) was built to explore tune both the friction force and adhesion energy simultaneously during the atomic simulations. In agreement with previous estimations, a wrinkle is easily formed under a lower frictional force and smaller adhesion. Finally, the influences of the ad-dimer in graphene and adatom on Cu substrate during the wrinkle formation process were discussed and it is found that a wrinkle always likes to be formed at the position of defect either in graphene or on the substrate and the critical strain can be greatly lowered by either the defects in graphene or those on the substrate. The wrinkle formation in single-layer graphene was studied in this paper. In the future, more complicated wrinkle formation in multi-layers graphene will be explored.

Acknowledgments

The authors acknowledge support from the Institute for Basic Science (IBS-R019-D1) of South Korea. The authors also acknowledge the usage of the IBS-CMCM high-performance computing system Cimulator.

Disclosure statement

No potential conflict of interest was reported by the authors.

Funding

This work was supported by the Institute for Basic Science of South Korea [IBS-R019-D1].

References

[1] Wang W, Yang S, Wang A. Observation of the unexpected morphology of graphene wrinkle on copper substrate. Sci Rep. 2017;7:1–6.
[2] Lee C, Wei X, Kysar JW, et al. Measurement of the elastic properties and intrinsic strength of monolayer graphene. science. 2008;321:385–388.
[3] Geim, A. K., Novoselov, K. S. The rise of graphene. Nature Mater. 2007;6:183–191.
[4] Balandin AA. Thermal properties of graphene and nanostructured carbon materials. Nat Mater. 2011;10:569–581.
[5] Balandin AA, Ghosh S, Bao W, et al. Superior thermal conductivity of single-layer graphene. Nano Lett. 2008;8:902–907.
[6] Nair RR, Blake P, Grigorenko AN, et al. Fine structure constant defines visual transparency of graphene. Science. 2008;320:1308.
[7] Aïssa B, Memon NK, Ali A, et al. Recent progress in the growth and applications of graphene as a smart material: a review. Front Mater. 2015;2:58.
[8] Ferrari AC, Bonaccorso F, Fal'Ko V, et al. Science and technology roadmap for graphene, related two-dimensional crystals, and hybrid systems. Nanoscale. 2015;7:4598–4810.
[9] Deng S, Berry V. Wrinkled, rippled and crumpled graphene: an overview of formation mechanism, electronic properties, and applications. Mater Today. 2016;19:197–212.
[10] Lee XJ, Hiew BYZ, Lai KC, et al. Review on graphene and its derivatives: synthesis methods and potential industrial implementation. J Taiwan Inst Chem Eng. 2019;98:163–180.
[11] Raccichini R, Varzi A, Passerini S, et al. The role of graphene for electrochemical energy storage. Nat Mater. 2015;14:271–279.
[12] Ren S, Rong P, Yu Q. Preparations, properties and applications of graphene in functional devices: a concise review. Ceram Int. 2018;44:11940–11955.
[13] Ogurtani OT, Senyildiz D, Cambaz Buke G. Wrinkling of graphene because of the thermal expansion mismatch between graphene and copper. Surf Interface Anal. 2018;50:547–551.
[14] Pang Z, Deng B, Liu Z, et al. Defects guided wrinkling in graphene on copper substrate. Carbon. 2019;143:736–742.
[15] Shaina PR, George L, Yadav V, et al. Estimating the thermal expansion coefficient of graphene: the role of graphene–substrate interactions. J Phys. 2016;28:085301.
[16] Yoon D, Son YW, Cheong H. Negative thermal expansion coefficient of graphene measured by Raman spectroscopy. Nano Lett. 2011;11:3227–3231.
[17] Hahn TA. Thermal expansion of copper from 20 to 800 K—standard reference material 736. J Appl Phys. 1970;41:5096–5101.
[18] Zhu W, Low T, Perebeinos V, et al. Structure and electronic transport in graphene wrinkles. Nano Lett. 2012;12:3431–3436.
[19] Nicholl RJ, Conley HJ, Lavrik NV, et al. The effect of intrinsic crumpling on the mechanics of free-standing graphene. Nat Commun. 2015;6:8789.
[20] Wang C, Liu Y, Li L, et al. Anisotropic thermal conductivity of graphene wrinkles. Nanoscale. 2014;6:5703–5707.
[21] Wang Y, Yang R, Shi Z, et al. Super-elastic graphene ripples for flexible strain sensors. ACS Nano. 2011;5:3645–3650.
[22] de Lima AL, Müssnich LA, Manhabosco TM, et al. Soliton instability and fold formation in laterally compressed graphene. Nanotechnology. 2015;26:045707.
[23] Li BW, Luo D, Zhu L, et al. Orientation-dependent strain relaxation and chemical functionalization of graphene on a Cu (111) foil. Adv Mater. 2018;30:1706504.
[24] Plimpton S. Fast parallel algorithms for short-range molecular dynamics (No. SAND-91-1144). Albuquerque, NM (United States): Sandia National Labs.; 1993.
[25] Zhang K, Arroyo M. Adhesion and friction control localized folding in supported graphene. J Appl Phys. 2013;113:193501.
[26] Zhang K, Arroyo M. Understanding and strain-engineering wrinkle networks in supported graphene through simulations. J Mech Phys Solids. 2014;72:61–74.

[27] Brenner DW, Shenderova OA, Harrison JA, et al. A second-generation reactive empirical bond order (REBO) potential energy expression for hydrocarbons. J Phys. 2002;14:783.
[28] Tersoff JJPRB. Modeling solid-state chemistry: interatomic potentials for multicomponent systems. Phys Rev B. 1989;39:5566.
[29] Brenner DW. Empirical potential for hydrocarbons for use in simulating the chemical vapor deposition of diamond films. Phys Rev B. 1990;42:9458.
[30] Martinez-Limia A, Zhao J, Balbuena PB. Molecular dynamics study of the initial stages of catalyzed single-wall carbon nanotubes growth: force field development. J Mol Model. 2007;13:595–600.
[31] Xu Z, Yan T, Ding F. Atomistic simulation of the growth of defect-free carbon nanotubes. Chem Sci. 2015;6:4704–4711.
[32] Foiles SM, Baskes MI, Daw MS. Embedded-atom-method functions for the fcc metals Cu, Ag, Au, Ni, Pd, Pt, and their alloys. Phys Rev B. 1986;33:7983.
[33] Jones JE. On the determination of molecular fields.—II. From the equation of state of a gas. Proc Royal Soc London. Ser A. 1924;106:463–477.
[34] Zhang X, Xu Z, Hui L, et al. How the orientation of graphene is determined during chemical vapor deposition growth. J Phys Chem Lett. 2012;3:2822–2827.
[35] Martyna GJ, Tuckerman ME, Tobias DJ, et al. Explicit reversible integrators for extended systems dynamics. Mol Phys. 1996;87:1117–1157.
[36] Li Z, Kinloch IA, Young RJ, et al. Deformation of wrinkled graphene. ACS Nano. 2015;9:3917–3925.
[37] Deng B, Pang Z, Chen S, et al. Wrinkle-free single-crystal graphene wafer grown on strain-engineered substrates. ACS Nano. 2017;11:12337–12345.
[38] Wang ZJ, Weinberg G, Zhang Q, et al. Direct observation of graphene growth and associated copper substrate dynamics by in situ scanning electron microscopy. ACS Nano. 2015;9:1506–1519.
[39] Chae SJ, Güneş F, Kim KK, et al. Synthesis of large-area graphene layers on poly-nickel substrate by chemical vapor deposition: wrinkle formation. Adv Mater. 2009;21:2328–2333.